Proceedings of ICAPP '12
Chicago, IL USA, June 24-28, 2012
Paper 12313

MODELING ANALYSIS FOR GROUT HOPPER WASTE TANK

Si Y. Lee
Computational Sciences
Savannah River National Laboratory
Aiken, SC 29808
Phone: (803) 725-8462, *Fax: (803) 725-8829*
si.lee@srnl.doe.gov;

Jason M. Ryans
Mercer University, Macon, GA 31207
Phone: (813) 389-3676, *jasonmichaelryans@gmail.com*

ABSTRACT – The Saltstone facility at Savannah River Site (SRS) has a grout hopper tank to provide agitator stirring of the Saltstone feed materials. The tank has about 300 gallon capacity to provide a larger working volume for the grout nuclear waste slurry to be held in case of a process upset, and it is equipped with a mechanical agitator, which is intended to keep the grout in motion and agitated so that it won't start to set up. The primary objective of the work was to evaluate the flow performance for mechanical agitators to prevent vortex pull-through for an adequate stirring of the feed materials and to estimate an agitator speed which provides acceptable flow performance with a 45^o pitched four-blade agitator. In addition, the power consumption required for the agitator operation was estimated.

The modeling calculations were performed by taking two steps of the Computational Fluid Dynamics (CFD) modeling approach. As a first step, a simple single-stage agitator model with 45^o pitched propeller blades was developed for the initial scoping analysis of the flow pattern behaviors for a range of different operating conditions. Based on the initial phase-1 results, the phase-2 model with a two-stage agitator was developed for the final performance evaluations. A series of sensitivity calculations for different designs of agitators and operating conditions have been performed to investigate the impact of key parameters on the grout hydraulic performance in a 300-gallon hopper tank. For the analysis, viscous shear was modeled by using the Bingham plastic approximation. Steady state analyses with a two-equation turbulence model were performed. All analyses were based on three-dimensional results. Recommended operational guidance was developed by using the basic concept that local shear rate profiles and flow patterns can be used as a measure of hydraulic performance and spatial stirring. Flow patterns were estimated by a Lagrangian integration technique along the flow paths from the material feed inlet.

I. INTRODUCTION

The Saltstone facility has a grout hopper tank of a 300 gallon capacity to provide agitator stirring of the Saltstone feed materials. The tank is equipped with a mechanical agitator, which is intended to keep the grout in motion so that it won't start to set up. The dry feeds and the salt solution are already mixed in the mixer prior to being transferred to the hopper tank. The hopper system is being designed for an adequate stirring of the mixed feed materials without a vortex-type pull-through. The agitator modeling study through this work will focus on fluid stirring and agitation, instead of traditional mixing in the literature, in order to keep the hopper contents such as grout in motion so that they will not be upset or solidified prior to transferring the grout to the Saltstone disposal facility. The hopper mixing system equipped with a mechanical agitator is schematically shown in Fig. 1.

A Computational Fluid Dynamics (CFD) modeling study was performed to evaluate the flow pattern behavior with a mechanical agitator and an estimate of the flow residence time in the grout hopper tank. The results of this study was used to develop the design guidelines for the agitator stirring of the Saltstone feed materials.

The objective of the work was to:

- Evaluate the nominal agitator speed under the baseline conditions in terms of satisfying the acceptance flow criteria during the stirring operation in the hopper.
- Perform a sensitivity analysis with respect to the baseline design and operating conditions such as agitator speeds, fluid levels, and fluid properties.

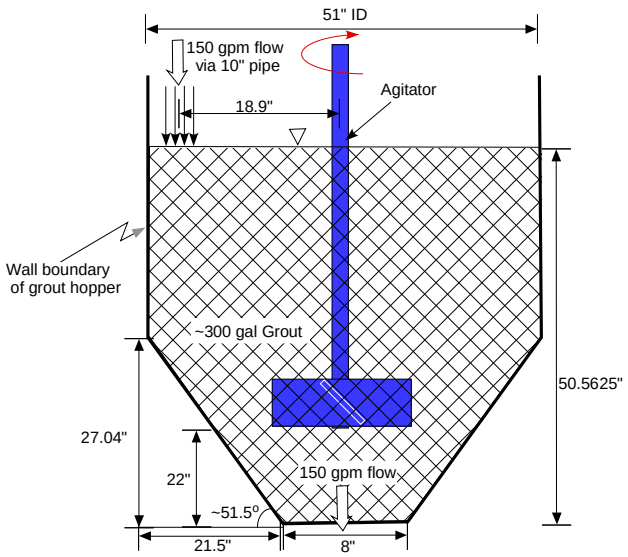

Fig. 1. Geometry of the agitator tank with pitched blades used for the phase-1 baseline modeling analysis

The primary goal of the work was to evaluate the flow stirring performance for mechanical agitators to prevent vortex pull-through and to estimate an agitator speed which provides acceptable flow performance with a 45° pitched four-blade agitator. In addition, the power consumption was estimated in a conservative way. The modeling results were used to develop the design guidelines for the agitator stirring of the Saltstone feed materials in a hopper tank.

For the modeling analysis, the flow patterns and shear rate profiles were primarily used as the performance acceptance criteria to allow adequate stirring prior to transfer of the hopper contents to the Saltstone processing facility. The criteria avoid a vortex-type pull-through flow patterns with stagnation zones inside the hopper so that the feed materials will get stirred in a reasonable way, and also is prevented from being solidified in regions such as near the hopper wall boundary during the stirring process.

The hopper modeling study consisted of two modeling stages. The first stage modeling study was based on a single-stage agitator with four 45° pitched flat-plate propeller blades for the initial phase-1 analysis. The modeling domain and agitator geometry for the phase-1 study are shown in Figs. 1 and 2. Based on the initial phase-1 results, the phase-2 modeling study was based on a two-stage agitator for the improved performance calculations. The two-stage agitator is shown in Fig. 3. As shown in the figure, the upper agitator has the 45° pitched propeller blades to promote the vertical fluid motion, and the lower one has the Rushton-type vertical blades to increase the fluid circulation in the radial direction. Each blade diameter for the phase-2 agitator is about two times larger than the phase-1 design to minimize the stagnation zone near the hopper wall boundary. The modeling conditions for the phase-1 and phase-2 modeling studies are provided in TABLE 1 and TABLE 2.

II. SOLUTION METHOD AND APPROACH

A three-dimensional CFD modeling method is used to achieve the objective. Based on the performance criteria discussed earlier, a steady-state computational approach was taken to compute flow fields driven by the agitator. The reference modeling conditions will be a 300-gallon hopper equipped with a four-blade flat propeller agitator with a 45° angle for the initial phase-1 baseline calculations. The geometrical configurations for the modeling domain are shown in Figs. 1 and 2. The modeling simulations used three-dimensional steady-state, isothermal governing equations with multiple reference frames.

For the numerical modeling and calculations, three-dimensional steady-state momentum and continuity equations were used as the basic governing equations to estimate fluid motion driven by an agitator with four 45° pitched blades. Hydraulic flow regime conditions were determined by estimating the Reynolds number corresponding to the operating conditions of a mechanical agitator considered for the Saltstone hopper modeling study. The laminar-turbulent transition occurred roughly around an impeller Reynolds number of 200.[1] When the Reynolds number is larger than 200, a standard two-equation turbulence model, referred to as κ–ε model in the literature, is used to capture turbulent eddy motion.

For incompressible steady-state flow, equation of the continuity is

$$\nabla \bullet \vec{v} = 0 \tag{1}$$

Equation of incompressible fluid motion is

$$\rho\left(\vec{v}\nabla\vec{v}\right) = -\nabla P + (\nabla \bullet \tau) + \rho\vec{g} \tag{2}$$

The Herschel-Bulkley equation combines the Bingham and power-law models assuming viscosity to be independent of shear rate with zero-shear yield stress. The equation type is

$$\tau = \tau_o + k\dot{\gamma}^{n} \tag{3}$$

where τ_o and k in Eq. (3) are yield stress and consistency, respectively. When n is equal to 1, and the transition region is assumed to be negligible, Eq. (3)

corresponds to the Bingham plastic model as shown in Fig. 2. As shown in the figure, consistency k becomes constant under the Bingham plastic model, that is, $k = \eta_\infty$.

$$\tau = \tau_o + \eta_\infty \dot{\gamma} \quad (4)$$

The transition region from shear-dependent viscosity to plastic viscosity of Newtonian fluid behavior was defined in implementing the Bingham plastic model in computational fluid dynamics approach. As shown in the figure, plastic viscosity η_∞ is found from the slope of the linear portion of the curve. Viscosity is the ability of a material to resist flow. Higher viscosity is characteristic of a less flowable suspension. The yield stress τ_o is determined by extending the linear portion of the curve to the vertical coordinate axis. It is the minimum stress required for a material to start flowing and deforming.

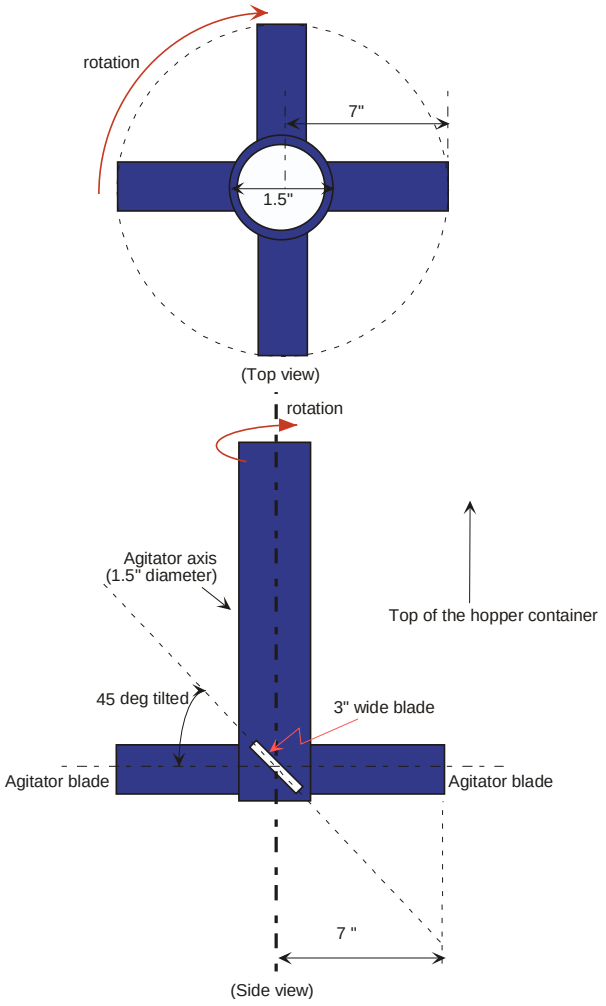

Fig. 2. Configurations of the single-stage agitator with four 45° pitched blades used for the phase-1 model

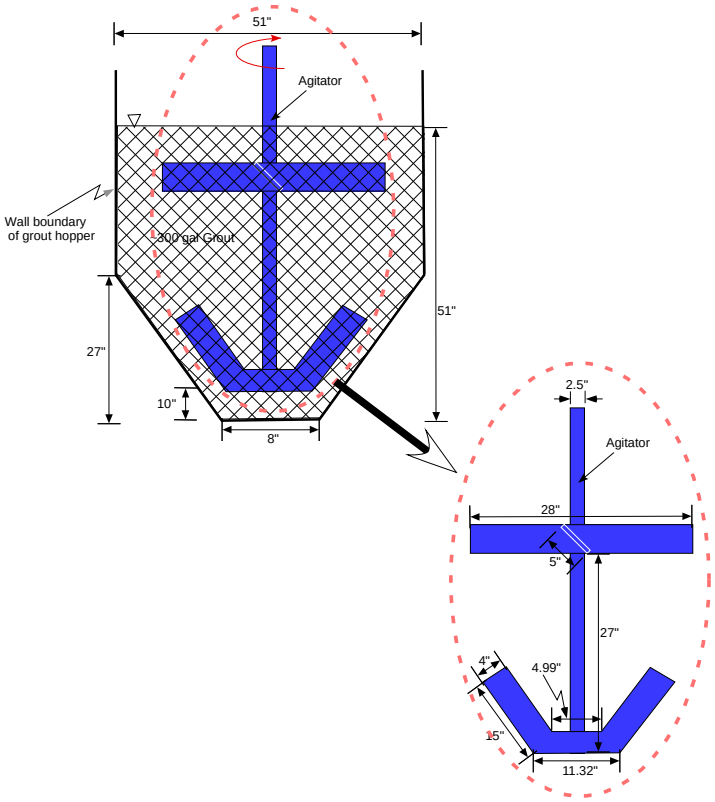

Fig. 3. Geometry of the agitator tank with two-stage blades used for the phase-2 modeling analysis

TABLE 1. Baseline modeling conditions used for the initial phase-1 analysis

Parameters		Modeling conditions
Hopper dimensions and agitator geometry		See Figs. 1 and 2
Agitator blade shape and type		Four flat blade and propeller type
Steady-state flow rate to the hopper tank, gpm		150
Number of agitator stages		Single stage
Each blade dimension, inches		7" long, 3" wide
Tank fluid level, inches		51
Blade elevation from the tank bottom, inches		22
Nominal baseline operating conditions	Agitator speed, rpm	175 (641 ft/min. tip speed)
	Fluid consistency, cp	42
	Fluid specific gravity	1.75
	Fluid yield stress, Pa	0.01*, 1*, 10*, 21.546 (0.45 lb_f/ft^2)

Note:*For sensitivity analysis

TABLE 2. Modeling conditions used for the phase-2 performance analysis

Parameters		Modeling conditions
Hopper dimensions and agitator geometry		See Fig. 3
Agitator blade shape and type		Four blade and 45-deg propeller type for upper one, four radial blade for lower one
Steady-state flow rate to the hopper tank, gpm		150
Number of agitator stages		Two stage
Each blade dimension, inches		14" long, 5" wide for upper blade, 15" long, 4" wide for lower blade
Tank fluid level, inches		51
Blade elevation from the tank bottom, inches		10, 6*
Nominal baseline operating conditions	Agitator speed, rpm	69.3 (508 ft/min.), 140 (1026 ft/min)* 200 (1466 ft/min)*
	Fluid consistency, cp	42
	Fluid specific gravity	1.75
	Fluid yield stress, Pa	1*, 5, 21.546*

Note:* For sensitivity analysis

The analysis consists of two major parts. One part is to calculate the phase-1 operating conditions (single stage agitator and 175 rpm agitator speed) by applying the Bingham plastic model to the agitated fluid domain for the initial estimate of flow patterns and flow residence time. The operating conditions and agitator geometry for the phase-1 calculations are provided in TABLE 1 and Fig. 2. The second part is to apply the phase-1 methodology to the modeling simulations and flow pattern analysis of the phase-2 agitator for various yield stresses and agitator speeds to evaluate the stirring performance of the phase-2 two-stage agitator as shown in Fig. 3. As shown in TABLE 3 and TABLE 4, the initial scoping results show that the flow domain driven by the phase-1 agitator is laminar in terms of an agitator Reynolds number, while the phase-2 flow domain is turbulent.

From two key turbulence parameters of k and ε, a quantity of turbulent eddy diffusivity (k^2/ε), can be formed without specification of flow-dependent mixing lengthscale λ.[2] When the turbulent energy transport term T' is modeled with a gradient-diffusion hypothesis as

TABLE 3. Flow conditions driven by the phase-1 baseline agitator shown in Fig. 2.

Pump speed		Agitator Reynolds number (Re_a)	Flow regime stirred by agitator
ft/min	rpm		
641	175**	~65	Laminar transition ($Re_a < 200$)
900	246	~90	

Note:* $Re_a = \left(\frac{\rho_f N D_B^{\,2}}{\mu_f} \right)$, where N is the revolution of agitator per unit time.
** Nominal speed

TABLE 4. Flow conditions driven by the phase-2 two-stage agitator shown in Fig. 3.

Pump speed		Agitator Reynolds number (Re_a)	Flow regime stirred by agitator
ft/min	rpm		
508	69.3**	~205	Turbulent transition ($Re_a > 200$)
1026	140	~413	
1466	200	~590	

Note:* $Re_a = \left(\frac{\rho_f N D_B^{\,2}}{\mu_f} \right)$, where N and D_B are the revolution of agitator per unit time and blade diameter, respectively.
** Nominal speed

$$T' = -\frac{\upsilon_T}{\sigma_k} \nabla k \tag{5}$$

where the turbulent Prandtl number for kinetic energy is generally taken to be $\sigma_k = 1.0$. In summary, the transport equation for turbulent kinetic energy k is

$$\frac{Dk}{Dt} = \nabla \bullet \left(\frac{\upsilon_T}{\sigma_k} \nabla k \right) + P - \varepsilon \tag{6}$$

The three other terms, $-Dk/Dt$, P, and ε, are in closed form given the turbulent-viscosity hypothesis.

Turbulence consists of high levels of fluctuating vorticity. At any instant, vortical motion called eddies are present in the flow. These eddies range in size from the largest geometrical scales of the flow such as tank diameter down to small eddies where molecular diffusion dominates. The eddies are continuously evolving, and the superposition of their induced motions leads to the fluctuating waves. In this situation, turbulent kinetic energy is dissipated from the largest

eddies down to the smallest through a process called energy cascade. In order to maintain the turbulence, a constant supply of energy must be fed to the turbulent fluctuations at the largest scales from the mean motions, where it is driven by a mechanical agitator. Thus, turbulent energy dissipation rate ε is viewed as the energy-flow rate in the cascade, and it is determined by the large-scale motions, independent of the viscosity at high Reynolds number. Consequently, the transport equation for ε is best considered as being entirely empirical. That is,

$$\frac{D\varepsilon}{Dt} = \nabla \bullet \left(\frac{\upsilon_T}{\sigma_\varepsilon} \nabla \varepsilon \right) + C_1 \left(\frac{\varepsilon}{k} \right) P - C_2 \frac{\varepsilon^2}{k} \qquad (7)$$

where the turbulent viscosity is

$$\upsilon_T = C_\mu \frac{k^2}{\varepsilon} \qquad (8)$$

where $C_\mu = 0.09$.

It is noted that the turbulent viscosity coefficient C_μ of 0.09 in the two-equation model (Eq. (8)) can be derived under the log-law.[3] From these results, the two-equation turbulence model, referred to as κ-ε model in the literature, was shown to be good for the bulk flow region including the log-law shear region as shown in the previous work.[4]

Based on the performance criteria as discussed earlier, a three-dimensional CFD approach was taken to compute flow fields driven by a mechanical agitator. The governing equations as described previously were solved simultaneously by using a commercial CFD code, FLUENT™.[5] A prototypic geometry for the agitator and hopper tank was created by a non-orthogonal control volume method in the CFD computational environment.

The analyses were based on the steady-state model for computational efficiency. The main solution methodologies and modeling assumptions were as follows:

- The fluid temperature was isothermally kept at 24 ^{o}C, neglecting the hydration heat generation of the cementitious material during the agitator stirring process.
- The fluid was assumed to be single-phase flow.
- The fluid behavior was assumed to follow the Bingham plastic model as discussed earlier.
- The present model was based on the 45^{o} pitched four-blade agitator and tank with no internal solid structures.
- The modeling simulations used three-dimensional steady-state governing equations with multiple reference frames (MRF).
- For the steady-state model, the top liquid surface was assumed to be frictionless and flat.

As mentioned above, the steady-state model assumes that free surface remains flat and slip wall. If the agitator rotates in a clockwise direction (as viewed from above), a large axial convection flow moves upward due to the rotation of the pitched blade. When the liquid level becomes low enough to get air pull-through due to vortex formation near the tips of the agitator blades, air will be drawn into the blade zone. An empirical equation is available in the literature to estimate the minimum liquid level which prevents air entrainment into the blade zone of the agitator.[6] Using the empirical correlation for air entrainment through the vortex formation, the liquid level required to avoid air pull-through under the phase-2 agitator was estimated as a function of agitator speed. The results show that when about 15 in fluid level above the agitator blade is kept during the hopper tank operation with the rotating speeds of 69 to 200 rpm, air pull-through entrainment through the top fluid surface will not occur.

III. CALCULATION RESULTS AND DISCUSSIONS

The Saltstone hopper models have been developed by a CFD approach to evaluate the flow pattern behavior with a mechanical agitator and to estimate the flow residence time in the grout hopper tank. For the CFD modeling calculations, different agitator designs and configurations were considered for examining the impact of fluid stirring performance for the initial baseline configurations. As the performance criteria, shear rate profile and flow pattern were used as a key indicator of the grout material movement from the rotating agitator region into the remote wall boundary zone in the fluid domain of the hopper tank. If the shear rate for the grout materials gets smaller than 10^{-5} (1/sec), the materials will not be mixed adequately and may be solidified during the process period. Estimation of flow patterns was used as the degree of stirring efficiency from the grout material interaction with blade passage and from the residence time of the tank contents to prevent vortex-type pull-through. The flow pattern was estimated from the flow path lines of the feed materials obtained by Lagrangian integration along the fluid movement starting from the material feed inlet.

As mentioned previously, the work used two modeling steps for the modeling calculations. One step is to develop a simple single-stage agitator tank model as an initial phase-1 approach to evaluate the initial scoping calculations and to provide design guideline for next phase agitator. It consists of 45^{o} pitched, four flat-plate blades. And each blade has 14 in diameter. The other is

to develop the phase-2 agitator model to conduct the stirring performance and sensitivity analyses, including the estimate of power consumptions. The computational meshes for the baseline phase-1 and phase-2 modeling domains to be used for the final analysis are presented in Fig. 4. Nominal design and operating conditions for the pahse-1 and phase-2 agitators used for the hopper tank modeling and analysis are provided in TABLE 1 and TABLE 2. Based on the modeling domains and operating conditions, the flow pattern calculations were performed. When 150 gpm material flows into the hopper tank through the 10-in pipe at top left corner and exits via the 8-in tank bottom, the computational models were run in steady state mode for a rotating agitator to allow the stirred flow profile to develop steady-state flow pattern. TABLE 5 shows all cases considered for the present modeling analysis.

III.A Phase-1 Modeling results

As discussed earlier, a single-stage hopper design was selected as the phase-1 agitator configuration, since a single propeller-type agitator is available for the initial calculations in stirring up the grout materials. Figure 5 shows typical flow patterns and stream path lines driven by the propeller blades as observed by numerical simulations for the phase-1 model. The path lines were obtained by Lagrangian integration along the flow motion. The results show that the rotating agitator submerged in a stationary hopper generates two primary flow motions consisting of axial convective flow from the 45° pitched flat surface and vortex flow at the tip of blade. The modeling results are consistent with the literature results.[1] When the material yield stress increases from 1 Pa to the baseline value of 21 Pa, flow patterns are significantly changed in terms of local velocity and flow path lines. It is indicated that when the yield stress becomes higher, the fluid become less affected by the agitator passage due to the higher shear stress as shown in Eq. (5). The shear rate profiles for various yield stresses are compared in a quantitative way in Fig. 6 when the phase-1 agitator mixes the hopper materials. The results show that the initial phase-1 single-stage agitator does not provide adequate stirring performance in terms of flow performance criteria since shear rates decreases rapidly for yield stresses larger than 10 Pa and they are well below 10^{-5} (1/sec) for the remote zone outside the 14-in agitator domain as shown in Fig. 6.

Figure 7 quantitatively compares shear stresses for a range of yield stresses (from 1 to 21 Pa). As shown in the figure, the modeling results clearly indicate that the tip of each agitator blade has the highest shear stress since its shear rate is the highest as presented in Fig. 6. The shear stress at the blade wall is closely related to the erosion characteristics of agitator blades and tank wall. These results are consistent with the literature information.[1,7]

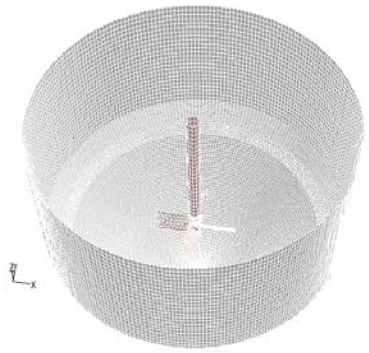

Baseline model (0.75 million meshes)

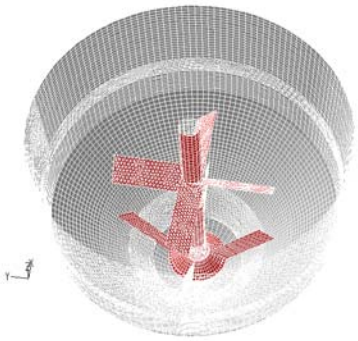

Phase-2 model (1.0 million meshes)

Fig. 4. Computational volume meshes used for the phase-1 and phase-2 models

Sensitivity analysis for different agitator speeds was performed for the assessment of the fluid movement generated by the phase-1 single-stage agitator. Shear rate profiles for the two different agitator speeds under maximum yield stress (21 Pa) are compared along the horizontal line A-A' crossing the agitator blade in Fig. 8. As shown in the figure, fluid movement for the remote region was not affected by the increase of the agitator speed for high yield stress. However, the modeling results show that when fluid yield stress becomes smaller, shear rates are affected significantly, especially, near the wall boundary region.

The phase-1 modeling study was based on the open tank system, which feeds the materials into the tank from the top left corner and discharges via the tank bottom at the same rate as the inlet. All the phase-1 results indicate that when yield stress of the Saltstone feed materials is higher than 10 Pa, the size of the agitator blade has to be increased for the enhancement of the shear rates near the hopper wall to prevent the solidification of the grout materials during the stirring operation. In this case, the power consumption P for keeping the feed materials of flowrate Q in motion is directly related to the blade size D_B. When the agitator speed is N revolutions per unit time, the power P becomes

$$P = 0.5 Q \rho_f (\pi N D_B)^2 \quad (9)$$

The results for the phase-1 baseline modeling calculations are summarized as follows:

- The modeling results clearly show that when the tank fluid has a higher viscosity, more fluid in the tank was unaffected by the blade passage and that the vortex system was not shed efficiently by the agitator blade.
- The flow patterns for the viscous fluid with high yield stress indicated very little disturbance of the fluid in the wall boundary or the clearance area near the wall.

Based on the initial phase-1 results, key parameters for the next phase agitator design are listed for keeping the hopper contents in motion prior to their transfer to the Saltstone processing facility. They are as follows:

- Blade size needs to be longer and wider to increase the impact of the agitator passage on fluid disturbance toward the wall boundary region remote from the agitator. The size of the agitator should be optimized by its power requirement as defined by Eq. (9).
- When the cementitious fluid has a high yield stress, a two-stage agitator consisting of radial blades and propeller blades is required to keep tank fluid in motion and longer fluid residence time.

III.B Phase-2 Modeling Results

Based on the initial phase-1 results, a two-stage agitator with longer and wider blades was selected for the phase-2 performance analysis. The agitator consists of the upper and lower agitator blades as shown in Fig. 3. As shown in the figure, the upper one has four 45^o pitched propeller blades, and the lower has four vertical flat-plate radial blades. For the performance analysis, the flow patterns and shear rate profiles were primarily used as the flow acceptance criteria to allow adequate stirring prior to transfer of the hopper contents. The criteria will minimize stagnation zones inside the hopper so that the feed materials are mixed and prevented from being solidified in a reasonable way during the stirring process.

As shown in TABLE 2, the performance calculations for two different heights of agitator, 10 and 6 inches above tank bottom, were conducted to examine the impact of agitator elevation on the stirring performance for given agitator configurations, keeping the 27 inch distance between impellers fixed as shown in Fig. 3. The phase-2 agitator located 10 in above the tank bottom exit was used as the phase-2 baseline modeling case. For a given agitator elevation, three different agitator speeds, 140 and 200 rpm, and the reference speed of 69.3 rpm, were considered for the assessment of the speed impact on the tank stirring performance for a range of fluid yield stresses in terms of flow patterns and shear rates. Shear rates and viscous stresses for the modeling domain were calculated from the simultaneous solutions of the flow governing equations combined with Bingham plastic equation as a constitutive relation for viscosity. The results were provided for the operation and design guidelines of the hopper tank system.

For the agitator speed of 69.3 rpm and the agitator elevation of 10 inches above the tank bottom, the baseline calculations for the phase-2 agitator were performed for a range of yield stresses (from 1 to 21 Pa). For the phase-2 performance analysis, 5 Pa yield stress was used as the baseline and nominal yield stress. Figure 9 compares the flow velocity distributions for the 150 gpm inlet flowrate for various yield stresses at 69.3 rpm agitator speed. The calculation results clearly indicate that as the yield stress becomes smaller than 5 Pa, shear rate for 69 rpm rotational speed increased rapidly near the tank wall region so that the agitator keeps fluid in motion more efficiently toward the remote region.

Sensitivity analysis for the agitator speed was performed to investigate the impact on the flow patterns for the same baseline operating conditions of case B1 other than the speed. The results show that when the agitator speed increases from the baseline value of 69.3 rpm to 140 rpm, the fluid is kept in motion more actively in terms of the Lagrangian fluid path lines, compared to those of the baseline speed. The sensitivity results due to the changes of the agitator speed are compared in Fig. 10 in terms of flow pathlines. When the hopper contents has the baseline yield stress of 5 Pa, comparison of shear rate profiles for different agitator speeds are compared at the locations of the upper and lower blades in Fig. 11. As shown in these figures, the shear rates at the remote region of the hopper tank are increased by several order of magnitudes with the agitator speed increased from 69.3 rpm to 140 rpm. It is clearly shown that the increase of the agitator speed helps keep the tank contents circulated in larger fluid region.

When agitator elevation is changed from the baseline value of 10 inches above the bank bottom to the minimum level of 6 inches for various yield stresses, comparison of flow shear rates for different agitator speeds is made for a given yield stress of 5 Pa at two different locations for 6 in elevation of the phase-2 agitator in Fig. 12. When the agitator speed increases from the baseline speed of 69.3 rpm to 140 rpm for a given yield stress of 5 Pa, comparison of primary flow path lines and residence times of the feed materials with 5 Pa yield stress between two different elevations of the

phase-2 agitator was made. The results show that both the fluid residence times for both cases are about the same, about 75 seconds. The shear rate profiles of the feed materials with 5 Pa yield stress were compared between the two different elevations of the phase-2 agitator at the 39-in vertical location under two different agitator speeds. The modeling results show that the performance indicators, the flow pattern and material residence time, are not sensitive to the elevation of the agitator inside the hopper.

As discussed previously, the shear stress was computed by the Bingham plastic approximation for a given yield stress and plastic consistency, Eq. (6). The Saltstone material may not be fed into the hopper tank in a continuous way through the top left corner of the tank as modeling here. It was noted that when there is no feed flow into the hopper, the shear rate profile become symmetrical with respect to the agitator as expected.

When 150 gpm material flow of 5 Pa yield stress is continuously fed into the top left corner of the hopper via 10 in pipe, the calculation results show that the highest shear stress is at the tip of the blades as expected. The modeling results clearly indicate that the lager agitator size and the faster rotational speed are recommended for the increased propagation of agitated flow disturbance to the wall boundary, which increases the fluid residence time to prevent the feed fluid from being discharged without any stirring and increases the shear rates to avoid solidification of stagnant grout prior to transfer of the tank contents.

Power consumptions required to drive the agitator rapidly increases with the agitator size and speed increases. The power consumptions were computed from the shear and pressure forces for different agitator speeds. The computed power was nondimensionalized by the reference power calculated by the agitator speed and size as given by Eq. (9). The nondimensional power number was evaluated as a function of agitator speed for the baseline phase-2 agitator. The results are shown in Fig. 13. The results indicate that the phase-2 two-stage agitator needs 140 rpm speed for optimum operation, and the motor to drive the agitator requires about 1.5 HP power.

IV. CONCLUSIONS

The modeling calculations were performed by using the two modeling steps. As a first step, a single-stage agitator with four 45^{o} pitched flat-plate propeller blades was developed for the initial phase-1 analysis of the flow pattern behaviors for a range of different modeling conditions. Based on the initial phase-1 results, the phase-2 model was developed for a two-stage agitator for the improved performance calculations. The modeling results should be considered as scoping calculations since the model was not validated against test results.

A series of sensitivity calculations for different design of agitators and operating conditions have been performed to provide operational guidance for grout stirring in a 300-gallon hopper tank. In the analysis, the viscous shear was modeled by using the Bingham plastic approximation. Steady state three-dimensional analyses coupled with a two-equation turbulence model were performed by CFD method. Recommended operational guidance was developed assuming that local shear rates and flow patterns can be used as a measure of hydraulic performance and spatial dispersion affected by the blade passage.

The main conclusions drawn from the hopper tank modeling and calculations are as follows:

- The baseline results show that when the tank fluid has a higher yield stress, more fluid in the tank was unaffected by the blade passage and that the vortex system was not shed by the agitator blade.
- The flow patterns for high yield stress fluid show that there is little disturbance of the fluid in the clearance area near the wall. Thus, there is no forceable removal of material away from the tank wall boundary, which is distant from the agitated flow region.
- The phase-2 results show that when the tank fluid has a yield stress smaller than 21 Pa, more fluid in the tank was affected by the blade passage and that the vortex system was shed by the agitator blade in an efficient way.
- When the fluid is more viscous, the agitator speed has less impact on flow patterns, resulting in less vortex shedding into the stagnation zone. However, the updated two-stage agitator is much better than the single-stage baseline design in terms of flow residence time and fluid flow patterns.
- The modeling results for the phase-2 agitator design show that when the tank fluid has a turbulent flow regime, tank contents were affected by the blade passage for a wide range of yield stresses (21 to 1 Pa) and that the vortex system was shed by the agitator blade in an efficient way.
- The results show that when the phase-2 two-stage agitator is operated with the baseline speed of 69 rpm for the hopper modeling, vortex pull-through of the tank feed materials can be minimized.
- The preliminary results show that when the tank fluid has a yield stress smaller than 21 Pa, 140 rpm agitator speed is favorable in terms of flow patterns and power consumption.

ACKNOWLEDGMENTS

This work was funded by U.S. Department of Energy and performed at the Savannah River National Laboratory, which is operated by the Savannah River Nuclear Solutions.

NOMENCLATURE

A	Area
C_μ	Turbulent viscosity coefficient
D	Tank diameter
D_B	Blade diameter
ft	feet (= 0.3048 m)
g	Gravitational acceleration
gallon	volume unit, 1 gallon = 3.7854 x 10^{-3} m^3
H_c	Critical height to prevent air entrainment to the blade
k	Kinetic energy
N	Speed of agitator rotation (revolutions per unit time)
P	Turbulent production rate or power consumption
p	Pressure
Δp	Pressure drop
Q	Volumetric flow rate
x	Local distance along the x-axis
y	Local distance along the y-axis
z	Local distance along the z-axis
ρ_f	Fluid density
ν	Kinematic viscosity
τ	Shear stress
κ	Turbulent kinetic energy per unit mass
ε	Turbulent energy dissipation rate per unit mass
τ_o	Yield stress
T'	Turbulent energy transport
σ_k	Turbulent Prandtl number
η_∞	Plastic viscosity or consistency
$\dot{\gamma}$	Shear rate
μ	Dynamic viscosity
In	Inch (= 0.0254 m)
Fr	Froude number
Re	Reynolds number
rpm	Rotations per minute
SRS	Savannah River Site

REFERENCES

1. G. B. Tatterson, *Fluid Mixing and Gas Dispersion in Agitated Tanks*, McGraw-Hill, Inc., New York, (1991).
2. Jones, W. P. and Launder, B. E., 1972, "The Prediction of Laminarization with a Two-Equation Model of Turbulence", *Int. J. of Heat Mass Transfer*, vol. 15, pp. 301-314, (1972).
3. R. A. Dimenna, S. Y. Lee, andD. A. Tamburello, "Advance Mixing Models", SRNL-STI-2011-00026, Fubruary (2011).
4. S. Y. Lee, R. A. Dimenna, R. A. Leishear, D. B. Stefanko, "Analysis of Turbulent Mixing Jets in a Large Scale Tank", ASME *Journal of Fluids Engineering*, vol. 130, No. 1, pp. 011104, (2008).
5. *FLUENT*, Fluent, Inc., (2003).
6. V. E. Schrock, R. T. Revankar, R. Mannheimer, S. Y. Lee, and C-H Wang, "Critical Flow Through a Small Break on a Large Pipe with Stratified Flow", Lawrence Berkeley National Laboratory, LBL-18386, (1985).
7. S. Y. Lee, R. A. Dimenna, G. A. Taylor, "Erosion Evaluations of Slurry Mixer Tank with Computational Methods", 14th International Conference on Nuclear Engineering (ICONE14) sponsored by ASME and Japanese Society of Mechanical engineers (JSME), Paper No. ICONE14-89309, June (2006).

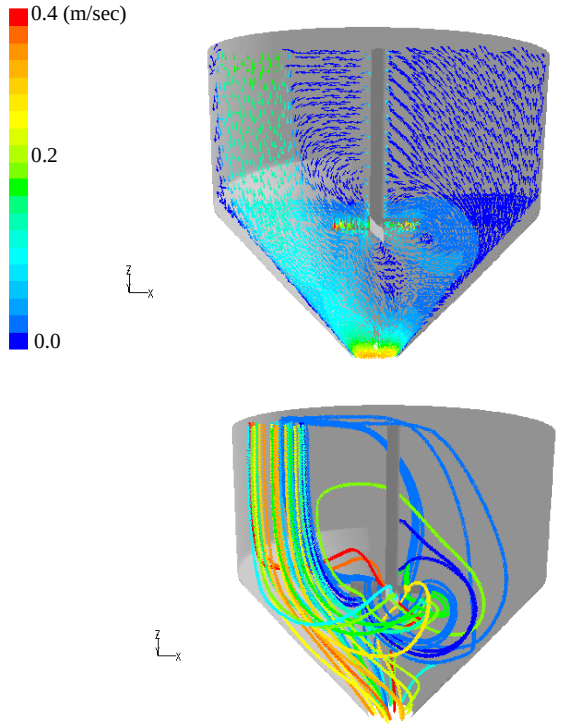

Fig. 5. Flow patterns and stream path lines for 1 Pa yield stress grout material inside the hopper tank with 175 rpm agitator speed.

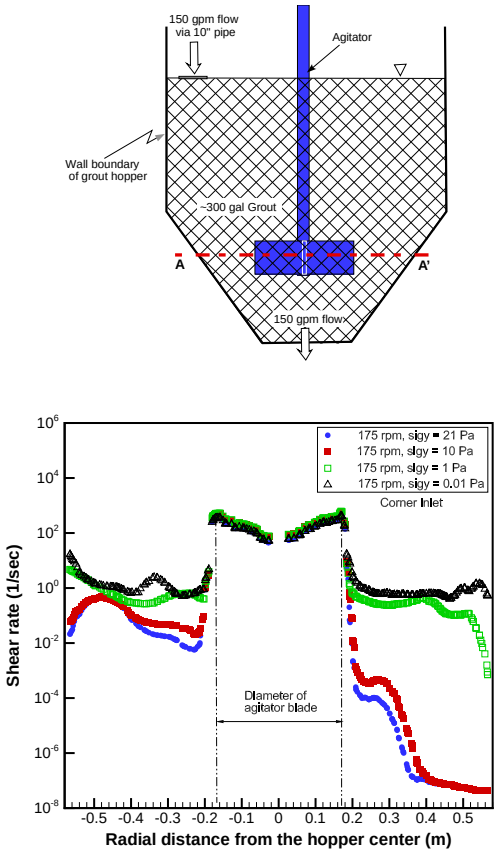

Fig. 6. Quantitative comparison of shear rates along the lin A-A' for various grout yield stresses under the phase-1 single-stage agitator with 175 rpm.

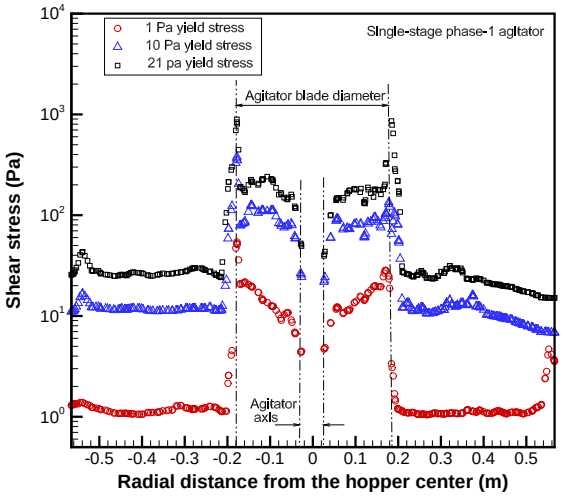

Fig. 7. Comparison of shear stresses along the horizontal line crossing the blades, line A-A' of Fig. 6, for various yield stresses inside the hopper tank with 175 rpm agitator speed with 150 gpm feed flow.

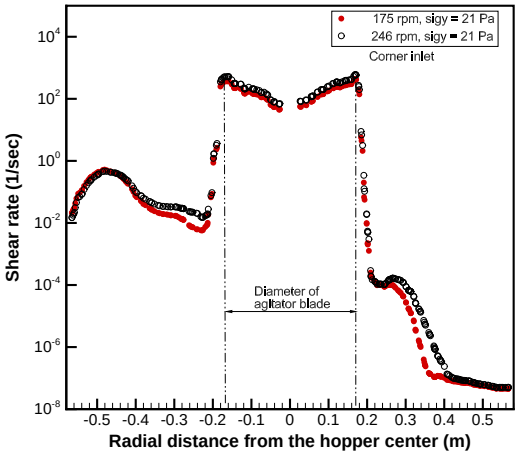

Fig. 8. Comparison of shear rates for the two different agitator speeds under the high yield stress (21 Pa) with 150 gpm feed flow along the horizontal line crossing the agitator blade

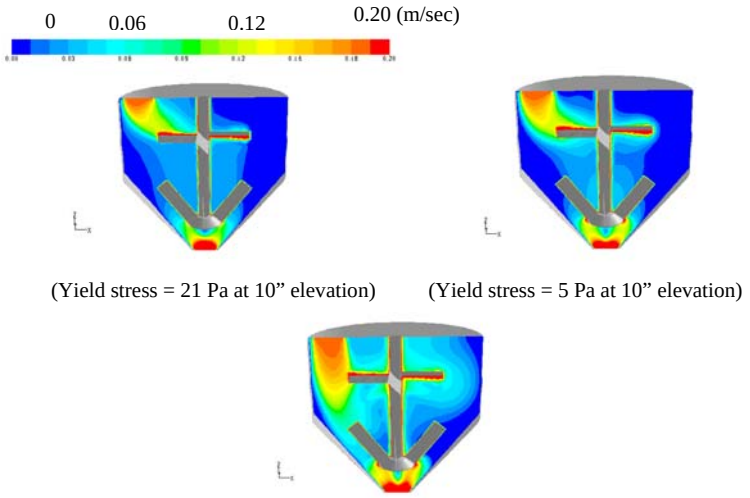

(Yield stress = 21 Pa at 10" elevation) (Yield stress = 5 Pa at 10" elevation)

(Yield stress = 1 Pa at 10" elevation)

Fig. 9. Velocity distributions for 150 gpm feed flowrate of the grout material through 10 in inlet pipe at top left corner under the phase-2 agitator speed of 69.3 rpm

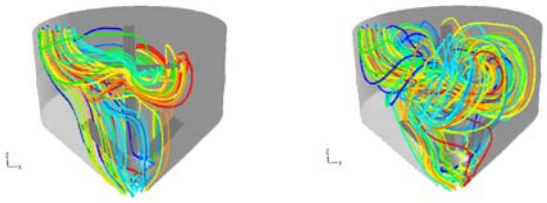

Fig. 10. Comparison of flow path lines of feed materials driven by the phase-2 agitator for two different speeds (10" agitator elevation, 5 Pa yield stress).

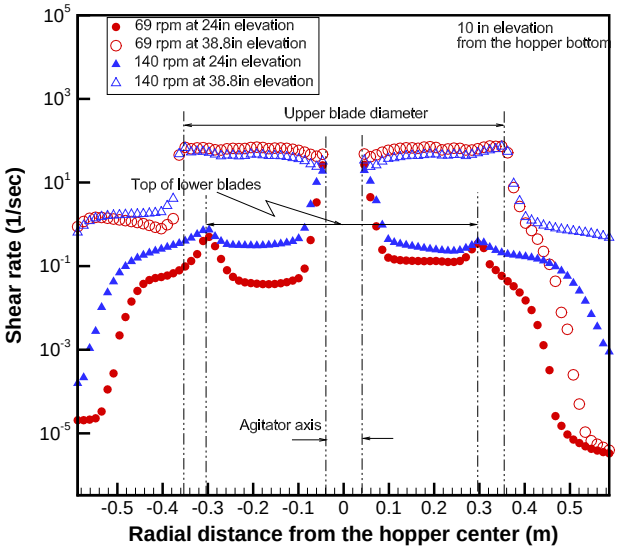

Fig. 11. Comparison of turbulent grout flow shear rates for different agitator speeds at different elevations under 5 Pa yield stress

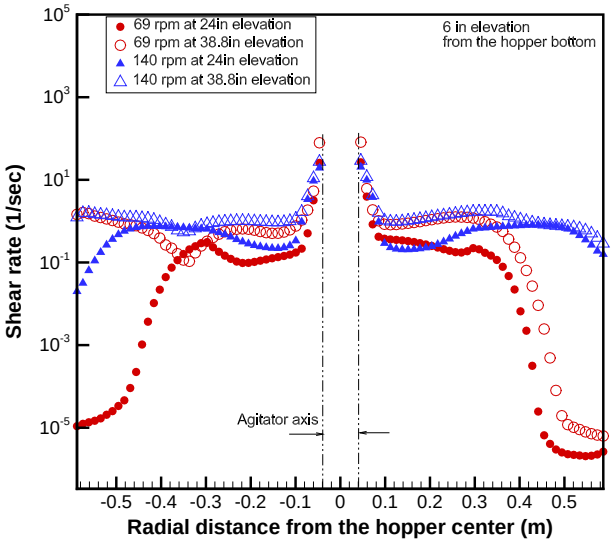

Fig. 12. Comparison of grout flow shear rates for different agitator speeds at different elevations under 5 Pa yield stress

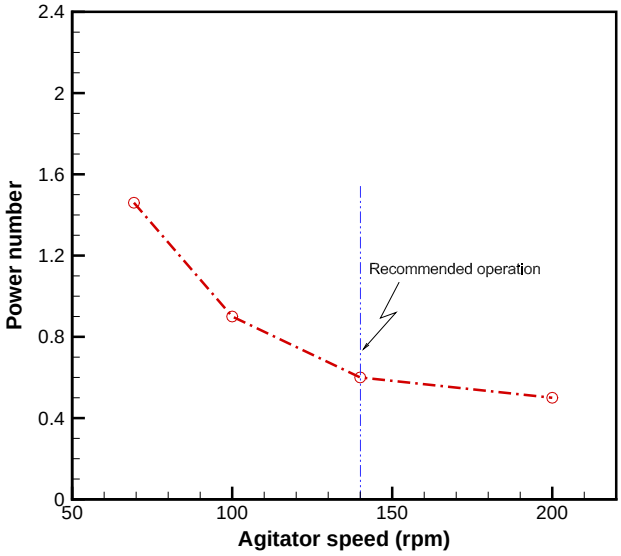

Fig. 13. Power consumptions and power number for various agitator speeds for 5 Pa yield stress materials